

Comparison of the diagnostic accuracy of FBP, ASiR, and MBIR reconstruction during CT angiography in the evaluation of a vessel phantom with calcified stenosis in a distal superficial femoral artery in a cadaver extremity

Jitsuro Tsukada (MD)^a, Minoru Yamada (PhD)^b, Yoshitake Yamada (MD, PhD)^a, Shun Yamazaki (MD)^c, Nobuaki Imanishi (MD, PhD)^d, Kentaro Tamura (MD)^a, Masahiro Hashimoto (MD)^a, Seishi Nakatsuka (MD, PhD)^a, Masahiro Jinzaki (MD, PhD)^{a,*}

Abstract

Purpose: To investigate whether adaptive statistical iterative reconstruction (ASiR) or model-based iterative reconstruction (MBIR) improves the diagnostic performance of computed tomography angiography (CTA) for small-vessel calcified lesions relative to filtered back projection (FBP) using cadaver extremities and a calcified stenosis phantom.

Methods: A cadaver was used in accordance with our institutional regulations, and a calcified stenosis phantom simulating 4 grades of stenosis was prepared. The phantom was inserted within the distal superficial femoral artery of the cadaver leg. Ten CT images per reconstruction type and stenosis grade were acquired using a 64-slice multidetector-row CTA.

As an objective measurement, the first and second derivatives of the CT value function profiles were calculated. As a subjective measurement, 2 blinded reviewers measured the stenosis ratio using a quantitative scale. The Wilcoxon rank-sum test was used to evaluate the data.

Results: Objective measurements of both 25% and 50% stenosis differed significantly ($P < 0.01$) between MBIR (25/50%: 25.80/50.30 \pm 3.88/3.86%) and FBP (25/50%: 35.60/83.80 \pm 3.44/26.10%), whereas significant differences were not observed between ASiR and FBP.

Reviewer 2's subjective measurements of 25% stenosis differed significantly ($P < 0.01$) between MBIR (35.13 \pm 3.25%) and ASiR (40.89 \pm 3.14%), and the measurements of 50% stenosis differed significantly ($P < 0.01$) between MBIR (reviewers 1/2, 62.36/54.78 \pm 2.78/4.96%) and FBP (reviewers 1/2, 62.36/74.84 \pm 2.78/18.10%). Significant differences in the subjective measurements were not observed between ASiR and FBP.

Conclusion: MBIR improves the diagnostic performance of CTA for small-vessel calcified lesions relative to FBP.

Abbreviations: ASiR = adaptive statistical iterative reconstruction, CTA = computed tomography angiography, FBP = filtered back projection, HU = Hounsfield units, IR = iterative reconstruction, MBIR = model-based iterative reconstruction, MDCT = multidetector-row CT, ROI = regions of interest, SAFIRE = sinogram affirmed iterative reconstructions, SFA = superficial femoral artery.

Keywords: dimensional measurement accuracy, image reconstruction, multidetector computed tomography, peripheral vascular diseases, vascular calcification

Editor: Zhonghua Sun.

The authors have no funding and conflicts of interest to disclose.

^a Department of Diagnostic Radiology, Keio University School of Medicine,

^b Multi-Dimension Biomedical Imaging and Information Laboratory in Research Park, Keio University School of Medicine, ^c Department of Plastic and Reconstructive Surgery, Keio University School of Medicine, ^d Department of Anatomy, Keio University School of Medicine, Tokyo, Japan.

* Correspondence: Masahiro Jinzaki, Department of Diagnostic Radiology, Keio University School of Medicine, Tokyo, Japan (e-mail: jinzaki@rad.med.keio.ac.jp).

Copyright © 2016 the Author(s). Published by Wolters Kluwer Health, Inc. All rights reserved.

This is an open access article distributed under the terms of the Creative Commons Attribution-Non Commercial-No Derivatives License 4.0 (CCBY-NC-ND), where it is permissible to download and share the work provided it is properly cited. The work cannot be changed in any way or used commercially.

Medicine (2016) 95:27(e4127)

Received: 2 March 2016 / Received in final form: 9 June 2016 / Accepted: 10 June 2016

<http://dx.doi.org/10.1097/MD.0000000000004127>

1. Introduction

Multidetector-row computed tomography angiography (CTA) of the lower extremity is recognized as an effective diagnostic tool for initial imaging tests in patients with suspected peripheral artery disease (PAD).^[1–4] Although, the diagnostic accuracy of 64-slice multidetector-row CT (MDCT) for noncalcified lesions has recently been reported to be as high as 98%,^[3] studies have shown that extensively calcified lesions tend to be overestimated because of the blooming effect, particularly in small-diameter arteries, such as coronary arteries and lower extremity arteries.^[5–10] Therefore, the accurate luminal stenosis evaluation of calcified small vessels remains a challenge, and the importance of spatial resolution and image noise has been acknowledged.^[8,10]

Currently, most clinical CT images are reconstructed by using the filtered back projection (FBP) technique. However, FBP has some limitations, such as the neglect of cone-beam geometry, the

data completeness problem, and the poor image quality in low-photon environments.^[11] Recently, iterative reconstruction (IR) techniques have become available, such as hybrid IR (adaptive statistical iterative reconstruction [ASiR], GE Healthcare, Waukesha, WI) and pure IR (model-based iterative reconstruction [MBIR], GE Healthcare). ASiR is the first generation of IR method that achieves both dose reduction and image quality improvement by decreasing the noise in reconstructed images.^[12] MBIR provides exact geometric features using a complex system of both backward and forward projections to iteratively match the reconstructed image to the acquired data based on the raw data, and it may improve image quality and spatial resolution, reduce streaking artifacts,^[13–16] and improve assessments of smaller vessels with calcified lesions due to the improved image quality.

These techniques are expected to provide better spatial resolution and less image noise than are provided by FBP. However, to the best of our knowledge, studies of small vessels with calcified lesions on lower extremity CTA have not focused on the use of these reconstruction techniques.

The purpose of our study was to investigate whether the use of MBIR improves the diagnostic performance of lower extremity CTA for small-vessel calcified lesions compared with that of FBP and ASiR. This experimental study used the bilateral lower extremities of a cadaver and a phantom with calcified stenosis.

2. Methods

2.1. Cadaver and phantom

This study is approved by the local ethics committee of our institute. The lower extremities of a fresh cadaver were obtained from the Willd Body Donation Program at the Department of Anatomy at our institution, and used in accordance with institutional regulations (the reference number is 20070026). The cadaver lower extremities were disarticulated at the hip joint, and the superficial femoral artery (SFA) and surrounding soft tissue remained intact.

A phantom consisting of calcified plaques, blood vessel lumen, and vessel walls that simulated 4 grades of calcified stenosis (normal diameter and 25%, 50%, and 75% stenosis) was also prepared (Fuyo Corporation, Tokyo, Japan) (Fig. 1). Calcified plaques were formed with hydroxyapatite with a CT attenuation of 1300 Hounsfield units (HU) at 120 kVp, and the results were close to those of highly calcified plaque.^[17] The blood vessel lumen was filled with an iodinated contrast material of 400 HU at 120 kVp, which is comparable to the lumen content obtained from clinical lower extremity CTA.^[18] The blood vessel wall was composed of acryl (100 HU at 120 kVp) with a thickness of 1.0 mm. The phantom, with a 3.0 mm internal diameter, corresponded to the size of the distal SFA.^[18] After opening the proximal end of the adductor canal, which courses between the anterior and medial compartment in the middle third of the thigh, the phantom was inserted within the distal SFA of the lower left extremity by using forceps. The space between the phantom, vessel, and surrounding tissue was filled with physiological saline before and after the phantom insertion procedure to remove air.

2.2. Image reconstruction and image noise measurement

The legs were positioned in parallel on the table of a 64-slice MDCT (Discovery CT750HD; GE Healthcare) and examined using the same scan parameters as our clinical lower extremity

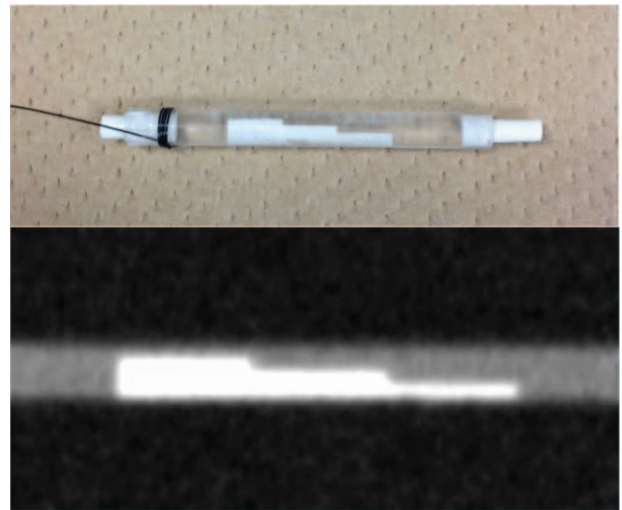


Figure 1. Phantom consisting of calcified plaques, blood vessel lumen, and vessel walls that simulated 4 grades of calcified stenosis (normal diameter, 25%, 50%, and 75%).

CTA protocol. Image acquisition was performed under automatic exposure control (50–500 mA tube current modulation) with a noise index of 10 (for a slice thickness of 5 mm). The other scanning parameters were as follows: collimation, 64 rows \times 0.625 mm; pitch, 1.375; gantry rotation, 0.5 s; and tube voltage, 120 kVp. The scan data were reconstructed in a 10 cm view field (512 \times 512 pixel matrix and 0.625 mm thickness) at a 0.625 mm interval using MBIR and an FBP standard kernel with 50% ASiR, wherein 50% of the ASiR images were blended with the FBP images. Continuous CT images were then selected at every 1.25 mm interval, and 10 CT images per 3 reconstruction types and 4 stenosis grades were acquired (Fig. 2).

Image noise was measured for all of the CT images. Circular regions of interest (ROIs; 10 mm diameter) were drawn in the fat and adductor magnus muscle, and the standard deviation for each ROI was calculated to estimate the image noise (Fig. 3). The size of each ROI was held constant for all of the CT images. The mean attenuation values and standard deviations were analyzed and selectively compared for each image reconstruction algorithm.

2.3. Objective measurement of the calcified stenosis with CT

All of the CT images were analyzed using image analysis software (ImageJ, National Institutes of Health, Washington, DC). The first and second derivatives of the CT value function profiles were calculated in terms of the vessel phantom stenosis rate.^[19] Each line of the CT value profile was placed at the same location on the 3 reconstruction images using the ImageJ macro program.

The lumen was detectable when the peaks of the first derivative showed positive values and the second derivative simultaneously showed 0 values; this result corresponds to the surrounding soft tissue/lumen border or the lumen/calcified lesion border. The lumen was also detectable when the peaks of the first derivative showed negative values and second derivative simultaneously showed 0 values; this result corresponds to the calcified lesion/surrounding soft tissue border. The lumen diameter was calculated, and a stenosis rate for every 120 views (10 axial

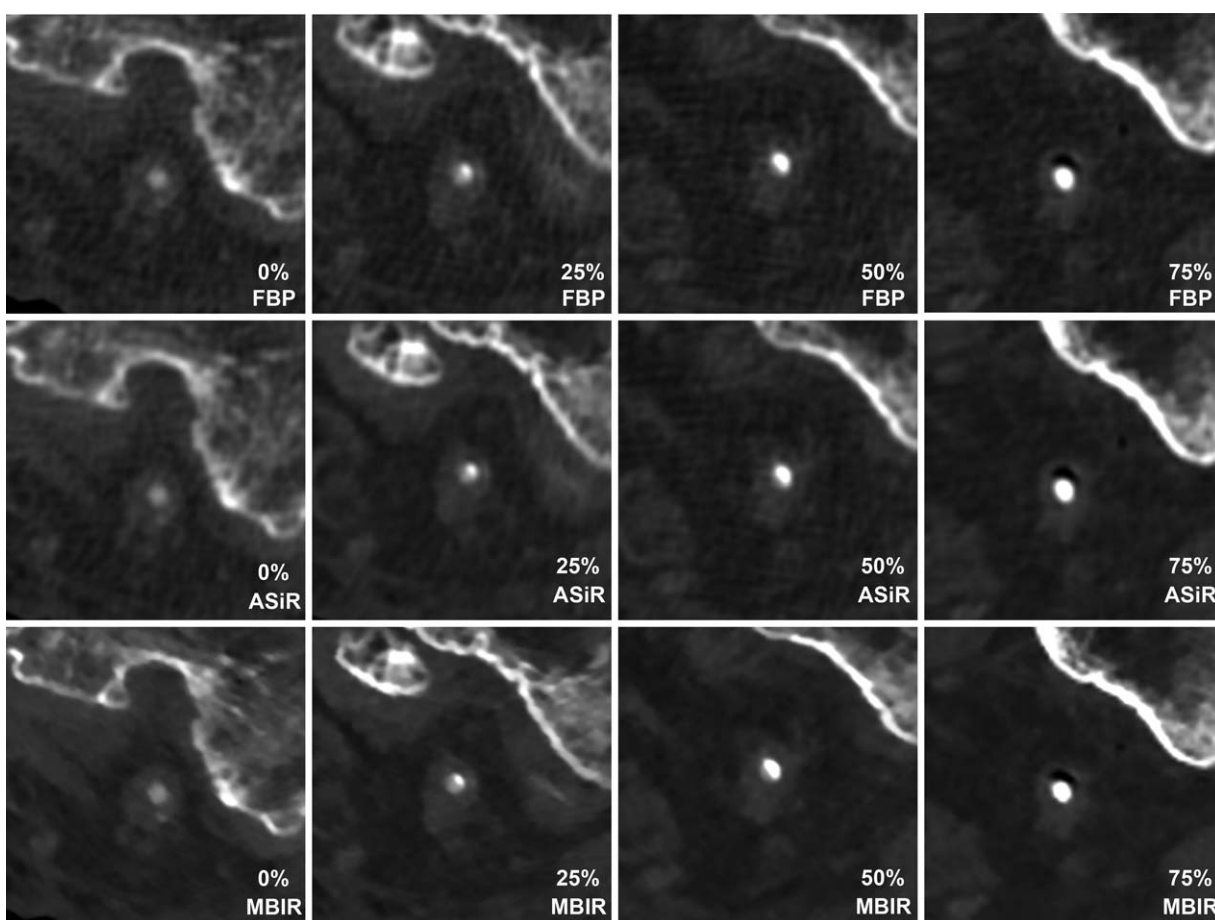


Figure 2. Reconstructed images of the vessel phantom within the distal superficial femoral artery of the cadaver's left lower extremity. ASiR=adaptive statistical iterative reconstruction, FBP=filtered back projection, MBIR=model-based iterative reconstruction.

views \times 4 stenosis grades \times 3 reconstruction algorithms) was calculated using the following formula: percent stenosis = $[(3 \text{ mm} - D_{\text{stenosis}})/3 \text{ mm}] \times 100$, where D_{stenosis} is the diameter of the lumen at the site of each stenosis.

2.4. Subjective measurement of the calcified stenosis with CT

All of the CT images were transferred to an offline workstation (OsiriX Medical Imaging Software, Pixmeo, Geneva, Switzerland) and numbered according to a random number generator. Two blinded reviewers worked independently at separate times and each viewed 120 randomized axial images. Each reviewer was a board-certified radiologist with 11 years of CT experience. The images were presented to the reviewers at the same window width (300 HU) and level (1000 HU); however, the reviewers were also encouraged to vary the window measurements at will. The reviewers received instructions for measuring the percent stenosis before performing their measurements, and they used a quantitative scale (from no stenosis to 100%) to subjectively evaluate the percent stenosis for each of the 120 images. No time limit was placed on the image review process.

2.5. Statistical analysis

Continuous measurements were expressed as means and standard deviations. The Wilcoxon signed rank-sum test with

Bonferroni correction was used to compare the objective and subjective measurements of the calcified stenosis and image noise from 3 reconstructed images. Interobserver agreement was evaluated by measuring the intraclass correlation coefficient. The statistical analyses were implemented using JMP software (version 11.0.0, SAS Institute Inc., Cary, NC). The significance level for all tests was 0.05 (2-sided).

3. Results

3.1. Reconstructed image and image noise

The calcified lesions on each reconstructed image were successfully demonstrated within the distal SFA of the left lower extremity (Fig. 3). Image noise from muscle and fat differed significantly ($P < 0.01$) among MBIR (fat/muscle: $16.80/17.80 \pm 3.21/3.21$), ASiR (fat/muscle: $20.40/21.40 \pm 1.75/3.24$), and FBP (fat/muscle: $23.80/24.40 \pm 3.21/4.32$).

3.2. Objective measurement of the calcified stenosis with CT

The first and second derivatives of the CT profiles function values were successfully calculated in terms of the vessel phantom stenosis rate (Fig. 4). Twenty-five percent stenosis was measured as 25.8% by MBIR, and the measured stenosis differed significantly ($P < 0.01$) between MBIR ($25.80 \pm 3.88\%$) and FBP ($35.60 \pm 3.44\%$, Fig. 5, Table 1). No significant difference

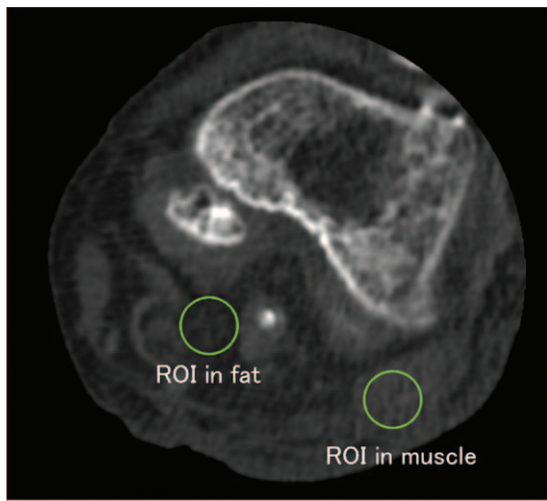


Figure 3. Evaluation of the image noise. Circular regions of interest (10 mm in diameter) were drawn in the femoral fat and adductor magnus muscle, and the standard deviation for each region of interest was calculated to estimate the image noise.

was observed between ASiR and FBP ($P=0.813$, Fig. 5). Fifty percent stenosis was measured as 50.3% by MBIR, and the measured stenosis differed significantly ($P < 0.01$) between MBIR ($50.30 \pm 3.86\%$) and FBP ($83.8 \pm 26.1\%$, Fig. 5, Table 1). No significant difference was observed between ASiR and FBP ($P=0.250$). Images of 75% stenosis were overestimated as 100% stenosis by all of the reconstruction techniques (FBR, ASiR, and MBIR, Table 1).

3.3. Subjective measurement of the calcified stenosis with CT

The results of the subjective measurements of percent stenosis are summarized in Table 2. Intraclass correlation coefficients ranged from 0.966 to 0.990, indicating high agreement between the 2 reviewers ($P < 0.01$, Table 2).

Twenty-five percent stenosis was measured as 32.8% to 39.8% stenosis by MBIR, whereas the 2 reviewers estimated it as 38.2% to 43.1% stenosis by ASiR and 36.9% to 44.7% stenosis by FBP (Table 2). For reviewer 2, the subjective measurements of 25% stenosis differed significantly ($P < 0.01$) between MBIR and ASiR (Fig. 6), whereas no significant difference was observed between ASiR and FBP. For reviewer 1, the accuracy of 25% stenosis by MBIR was greater than that by FBP; however, the difference was not statistically significant (Fig. 6).

Fifty percent stenosis was measured as 51.2% to 64.3% stenosis by MBIR by the 2 reviewers, whereas it was estimated as 61.3% to 78.4% stenosis by ASiR and as 61.9% to 87.8% stenosis by FBP (Table 2). The measured stenosis differed significantly (reviewer 1/2, $P=0.006/0.002$) between MBIR and FBP (Fig. 6), whereas no significant difference was observed between ASiR and FBP (reviewer 1/2, $P=0.910/0.275$).

Images of 75% stenosis were overestimated as 90% to 100% stenosis by all of the reconstruction techniques, and the measurements of percent stenosis showed no significant differences among MBIR, ASiR, and FBP (Table 2).

4. Discussion

In our study, MBIR showed significantly greater accuracy than did FBP in measuring for 50% stenosis in the objective and subjective measurements and for 25% stenosis in the objective measurements, indicating that MBIR provides higher diagnostic

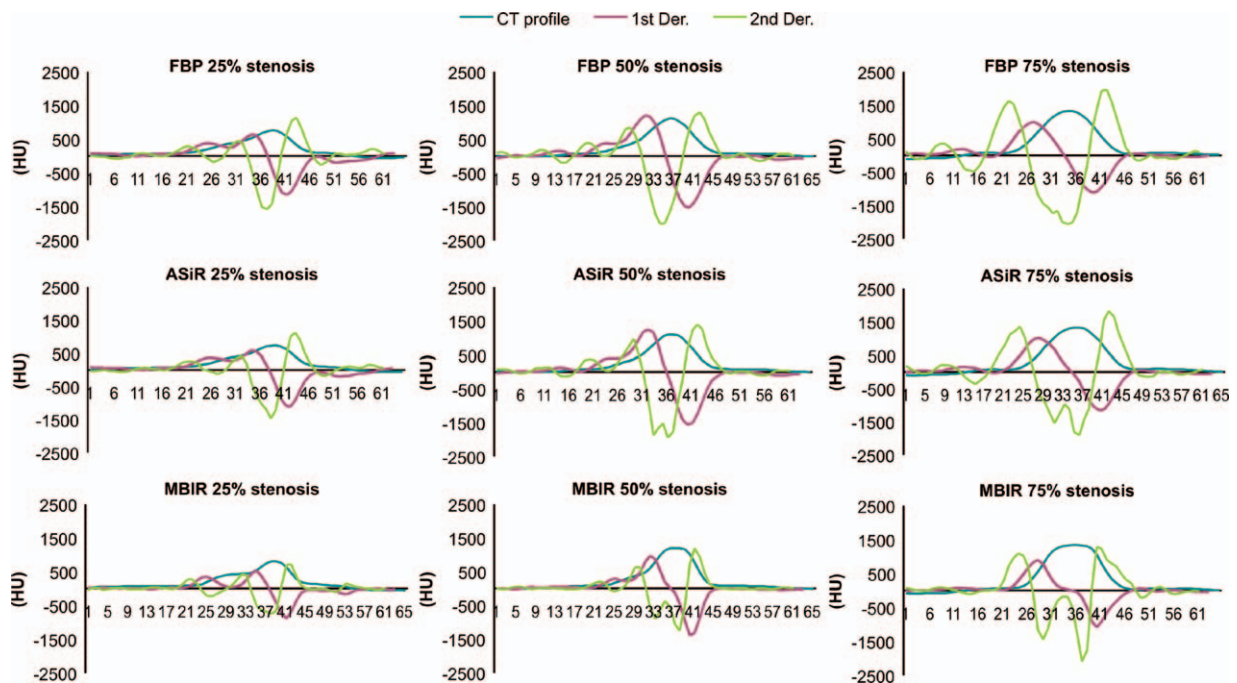


Figure 4. Objective measurement of the calcified stenosis. This graph shows the first (red line) and second (green line) derivatives of the computed tomography value profile (blue line) functions in terms of the stenosis ratio of the vessel phantom in each reconstruction algorithm. ASiR=adaptive statistical iterative reconstruction, Der.=derivative, FBP=filtered back projection, MBIR=model-based iterative reconstruction.

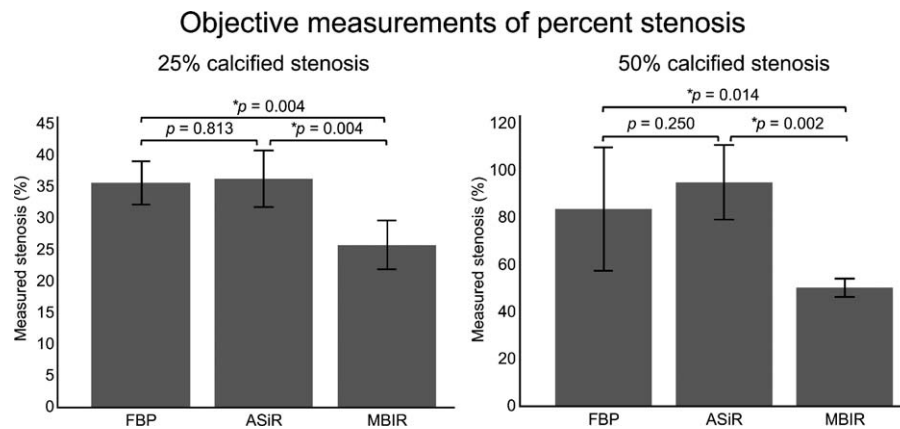


Figure 5. Objective measurement of 25% and 50% calcified stenosis of the vessel phantom. The bar graphs show the reconstruction method and objectively measured percent stenosis of the vessel phantom at 25% and 50%. Error bars indicate 1 standard deviation. Wilcoxon signed rank-sum test was used to objectively compare the measured 25% and 50% calcified stenosis between 3 reconstructed computed tomography images. $P < 0.017$ was considered to be statistically significant with Bonferroni correction for multiple comparisons. $*P < 0.017$. ASiR=adaptive statistical iterative reconstruction, FBP=filtered back projection, MBiR=model-based iterative reconstruction.

performance for small-vessel calcified lesions on lower extremity CTA compared with FBP. In particular, MBiR correctly diagnosed 50% stenosis, whereas conventional CTA with FBP has been shown to overestimate this percent stenosis as $>70\%$.^[2,7,20,21] These findings are important because MBiR may reduce the false-positive rate in calcified stenosis lesions using CTA, thereby avoiding unnecessary angiography.

One possible reason for the higher diagnostic accuracy of MBiR compared with FBP is that MBiR provides less image noise and better spatial resolution.^[13,16,22] A recent study using noncalcified and nonstenotic phantoms indicated that MBiR improves the accuracy of diameter measurements by CTA because backward and forward projections are used to iteratively match the reconstructed image to the acquired data according to system and statistical models, thereby offering better spatial resolution and less image noise than does FBP.^[15] Scheffel et al^[22]

reported that MBiR improved image quality and reduced image noise compared with FBP and ASiR by using ex vivo coronary artery. Moreover, some studies showed the superiority of improved image quality and reduced image noise of MBiR as compared with FBP in the evaluation of anterior spinal artery^[23] and coronary arteries.^[24]

IR also has been shown to reduce blooming artifacts due to beam hardening.^[10,25] Blooming artifacts from adjacent severely calcified lesion^[10] or implanted stents^[26,27] are contributed to the limited spatial resolution due to the spillover effect from high-attenuation structures. IR can selectively improve high contrast resolution without increasing image noise via the reconstruction algorithms, which reduces blooming artifacts. For example, Renker et al^[10] measured implanted stent volumes with volume analysis software to evaluate blooming artifacts, and the measured calcification volumes were significantly lower ($P = 0.019$) with IR compared with FBP. Ebersberger et al^[25] also reported that full-dose sinogram affirmed iterative reconstructions (SAFIRE; Siemens Healthcare) showed a significantly ($P < 0.05$) lower stent-lumen attenuation increase ratio, which is known as a marker for stent blooming artifacts, compared with that obtained with FBP. Therefore, the MBiR might be useful for evaluating small vessels such as peripheral arteries and coronary arteries.

In contrast, the results from our objective and subjective evaluations demonstrated that although ASiR can significantly reduce image noise, its diagnostic accuracy was not significantly different from that of FBP based on the objective and subjective results. Prakash et al^[28] reported that there was no significant difference between ASiR and FBP in the measurement of small bronchioles of the lungs, whereas ASiR-assisted high-definition kernels reconstruction yielded a superior visualization result compared with both ASiR and FBP. In a vessel study, Scheffel et al^[22] found no significant differences between FBP and ASiR with respect to image quality, image sharpness, or luminal CT number in the coronary artery. Although they suggested that the similar results between ASiR and FBP might have been due to their scoring system, other explanations are possible. Our results indicate that although ASiR is superior to FBP in reducing the noise associated with standard reconstruction algorithms, the spatial resolution and signal-to-noise ratio of ASiR are not as

Table 1
Objective measurement of calcified stenosis in the vessel phantom.

Reconstruction algorithm	Stenosis of the phantom, %	Measured stenosis, %
FBP	0	0
	25	35.60 ± 3.44
	50	83.80 ± 26.10
	75	100
ASiR	0	0
	25	36.30 ± 4.57
	50	95.00 ± 15.80
	75	100
MBiR	0	0
	25	25.80 ± 3.88*
	50	50.30 ± 3.86†
	75	100

Data are mean ± standard deviation.

ASiR=adaptive statistical iterative reconstruction, FBP=filtered back projection, MBiR=model-based iterative reconstruction.

*MBiR had a significantly higher accuracy than FBP ($P = 0.004$) and ASiR ($P = 0.004$) at 25% stenosis.

†MBiR had a significantly higher accuracy than FBP ($P = 0.014$) and ASiR ($P = 0.002$) at 50% stenosis. $P < 0.017$ was considered to be statistically significant with Bonferroni correction for multiple comparisons.

Table 2
Subjective measurement of calcified stenosis in the vessel phantom.

Reconstruction algorithm	Stenosis of the phantom, %	Measured stenosis				Intraclass correlation
		Blinded reviewer 1		Blinded reviewer 2		
		Mean, %	95% CI	Mean, %	95% CI	
FBP	0	0	0	0	0	0.966 ($P < 0.001$)
	25	41.64 ± 4.25	38.6–44.7	40.09 ± 4.42	36.9–43.2	
	50	71.71 ± 6.68	66.9–76.5	74.84 ± 18.1	61.9–87.8	
	75	99.02 ± 1.58	97.9–100.0	96.03 ± 8.43	90–102	
ASiR	0	0	0	0	0	0.973 ($P < 0.001$)
	25	40.65 ± 3.46	38.2–43.1	40.89 ± 3.14	38.6–43.1	
	50	71.95 ± 8.97	65.5–78.4	66.38 ± 7.10	61.3–71.4	
	75	95.73 ± 5.38	91.6–99.3	96.18 ± 8.06	90.4–102.0	
MBiR	0	0	0	0	0	0.990 ($P < 0.001$)
	25	37.26 ± 3.55	34.7–39.8	35.13 ± 3.25 [†]	32.8–37.5	
	50	62.36 ± 2.78 [*]	60.4–64.3	54.78 ± 4.96 [‡]	51.2–58.3	
	75	97.73 ± 2.64	95.8–99.6	100	0	

Data are mean ± standard deviation.

ASiR = adaptive statistical iterative reconstruction, CI = confidence interval, FBP = filtered back projection, MBiR = model-based iterative reconstruction.

^{*} MBiR had a significantly higher accuracy than FBP ($P = 0.006$) and ASiR ($P = 0.004$) at 50% stenosis.

[†] MBiR had a significantly higher accuracy than ASiR ($P = 0.01$) at 25% stenosis.

[‡] MBiR had a significantly higher accuracy than FBP ($P = 0.002$) and ASiR ($P = 0.004$) at 50% stenosis. $P < 0.017$ was considered to be statistically significant with Bonferroni correction for multiple comparisons.

high as those obtained with MBiR, which uses the accurate system model, the statistical noise model, and the prior model through the IR process.^[11,16] Moreover, the ability to reduce blooming artifacts in the presence of severe calcification might be lower for ASiR than for MBiR.

In our study, 75% stenosis was overestimated as 100% stenosis in the objective measurements and as 90% to 100% stenosis in the subjective measurements, even when using MBiR. This overestimation likely occurred because of the inability to eliminate the partial volume effect and blooming artifacts when using MBiR. There were 2 positive peaks in the first derivative at 25% and 50% stenosis, which corresponded to the border of surrounding soft tissue/lumen and lumen/calcification, respectively (Fig. 4). In contrast, the 2 peaks were not detected at 75% stenosis, even when using MBiR, likely because of blooming artifacts (Fig. 4). Thus, improved spatial resolution and further reduction of blooming artifacts might be required for more

accurate differentiation of severe stenosis (75% or 90%) in small-diameter arteries, which is important for selecting the interventional procedures.

Our study had several limitations. First, this experimental study used cadaver lower extremities. To establish whether MBiR can improve the diagnostic accuracy of small-vessel calcified lesions in patients with PAD, further investigations with live patients are required. Second, only 1 pair of cadaver lower extremities was obtained for our study because it is difficult to prepare multiple fresh cadavers at our institution. Third, although the image sets for each reconstruction technique were randomly presented, it was difficult to blind the observers because of differences in image appearance among reconstruction techniques. Finally, the diagnostic performance at different kVp settings was not evaluated in this study. Such performance, particularly at lower tube voltages, will be evaluated in a future study.

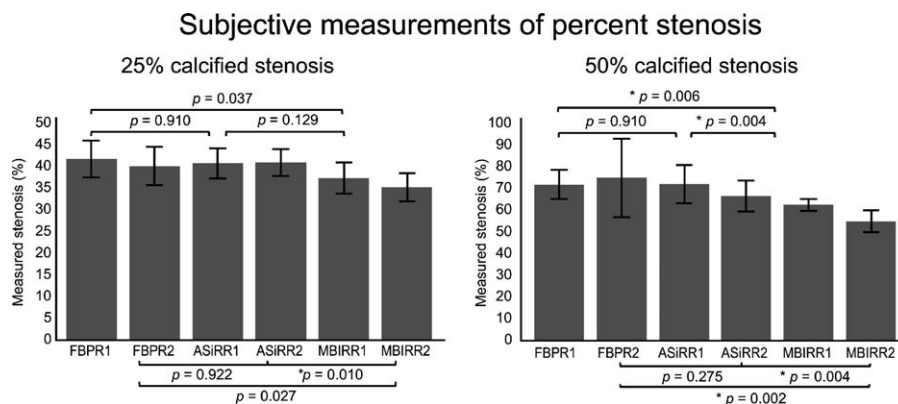


Figure 6. Subjective measurements of 25% and 50% calcified stenosis. The bar graphs show the reconstruction method and the subjectively measured percent stenosis of the vessel phantom at 25% and 50% by 2 reviewers. The error bars indicate 1 standard deviation. Wilcoxon signed rank-sum test was used to compare the subjectively measured 25% and 50% calcified stenosis among 3 reconstructed computed tomography images by 2 reviewers. $P < 0.017$ was considered to be statistically significant with Bonferroni correction for multiple comparisons. $*P < 0.017$. ASiR = adaptive statistical iterative reconstruction, FBP = filtered back projection, MBiR = model-based iterative reconstruction, R1 = reviewer 1, R2 = reviewer 2.

In conclusion, MBIR showed a higher diagnostic accuracy of small-vessel calcified lesions using lower extremity CTA compared with FBP.

References

- [1] Heijenbrok-Kal MH, Kock MC, Hunink MG. Lower extremity arterial disease: multidetector CT angiography meta-analysis. *Radiology* 2007;245:433–9.
- [2] Brockmann C, Jochum S, Sadick M, et al. Dual-energy CT angiography in peripheral arterial occlusive disease. *Cardiovasc Intervent Radiol* 2009;32:630–7.
- [3] Napoli A, Anzidei M, Zaccagna F, et al. Peripheral arterial occlusive disease: diagnostic performance and effect on therapeutic management of 64-section CT angiography. *Radiology* 2011;261:976–86.
- [4] Sun Z. Diagnostic accuracy of multislice CT angiography in peripheral arterial disease. *J Vasc Interv Radiol* 2006;17:1915–21.
- [5] Kau T, Eicher W, Reiterer C, et al. Dual-energy CT angiography in peripheral arterial occlusive disease-accuracy of maximum intensity projections in clinical routine and subgroup analysis. *Eur Radiol* 2011; 21:1677–86.
- [6] Sarwar A, Rieber J, Mooyaart EA, et al. Calcified plaque: measurement of area at thin-section flat-panel CT and 64-section multidetector CT and comparison with histopathologic findings. *Radiology* 2008;249:301–6.
- [7] Willmann JK, Baumert B, Schertler T, et al. Aortoiliac and lower extremity arteries assessed with 16-detector row CT angiography: prospective comparison with digital subtraction angiography. *Radiology* 2005;236:1083–93.
- [8] Ouwendijk R, Kock MC, van Dijk LC, et al. Vessel wall calcifications at multi-detector row CT angiography in patients with peripheral arterial disease: effect on clinical utility and clinical predictors. *Radiology* 2006;241:603–8.
- [9] Yim PJ, Noshier JL, Burgos A, et al. Subtraction computed tomographic angiography of calcified arteries: preliminary phantom and clinical studies. *Academic Radiol* 2009;16:257–65.
- [10] Renker M, Nance JW Jr, Schoepf UJ, et al. Evaluation of heavily calcified vessels with coronary CT angiography: comparison of iterative and filtered back projection image reconstruction. *Radiology* 2011;260:390–9.
- [11] Thibault JB, Sauer KD, Bouman CA, et al. A three-dimensional statistical approach to improved image quality for multislice helical CT. *Med Phys* 2007;34:4526–44.
- [12] Singh S, Kalra MK, Gilman MD, et al. Adaptive statistical iterative reconstruction technique for radiation dose reduction in chest CT: a pilot study. *Radiology* 2011;259:565–73.
- [13] Nishida J, Kitagawa K, Nagata M, et al. Model-based iterative reconstruction for multi-detector row CT assessment of the Adamkiewicz artery. *Radiology* 2014;270:282–91.
- [14] Vardhanabhuti V, Ilyas S, Gutteridge C, et al. Comparison of image quality between filtered back-projection and the adaptive statistical and novel model-based iterative reconstruction techniques in abdominal CT for renal calculi. *Insights Imaging* 2013;4:661–9.
- [15] Suzuki S, Machida H, Tanaka I, et al. Vascular diameter measurement in CT angiography: comparison of model-based iterative reconstruction and standard filtered back projection algorithms in vitro. *AJR Am J Roentgenol* 2013;200:652–7.
- [16] Yamada Y, Jinzaki M, Tanami Y, et al. Model-based iterative reconstruction technique for ultralow-dose computed tomography of the lung: a pilot study. *Invest Radiol* 2012;47:482–9.
- [17] Brodoefel H, Burgstahler C, Heuschmid M, et al. Accuracy of dual-source CT in the characterisation of non-calcified plaque: use of a colour-coded analysis compared with virtual histology intravascular ultrasound. *Br J Radiol* 2009;82:805–12.
- [18] Li XM, Li YH, Tian JM, et al. Evaluation of peripheral artery stent with 64-slice multi-detector row CT angiography: prospective comparison with digital subtraction angiography. *Eur J Radiol* 2010;75:98–103.
- [19] Yamada M, Jinzaki M, Tanami Y, et al. Detection of a coronary artery vessel wall: performance of 0.3 mm fine-cell detector computed tomography—a phantom study. *Phys Med Biol* 2011;56:5235–47.
- [20] Meyer BC, Werncke T, Hopfenmuller W, et al. Dual energy CT of peripheral arteries: effect of automatic bone and plaque removal on image quality and grading of stenoses. *Eur J Radiol* 2008;68:414–22.
- [21] Albrecht T, Foert E, Holtkamp R, et al. 16-MDCT angiography of aortoiliac and lower extremity arteries: comparison with digital subtraction angiography. *AJR Am J Roentgenol* 2007;189:702–11.
- [22] Scheffel H, Stolzmann P, Schlett CL, et al. Coronary artery plaques: cardiac CT with model-based and adaptive-statistical iterative reconstruction technique. *Eur J Radiol* 2012;81:e363–9.
- [23] Machida H, Takeuchi H, Tanaka I, et al. Improved delineation of arteries in the posterior fossa of the brain by model-based iterative reconstruction in volume-rendered 3D CT angiography. *AJNR Am J Neuroradiol* 2013;34:971–5.
- [24] Fuchs TA, Stehli J, Bull S, et al. Coronary computed tomography angiography with model-based iterative reconstruction using a radiation exposure similar to chest X-ray examination. *Eur Heart J* 2014;35: 1131–6.
- [25] Ebersberger U, Tricarico F, Schoepf UJ, et al. CT evaluation of coronary artery stents with iterative image reconstruction: improvements in image quality and potential for radiation dose reduction. *Eur Radiol* 2013;23: 125–32.
- [26] Tanami Y, Jinzaki M, Yamada M, et al. Improvement of in-stent lumen measurement accuracy with new high-definition CT in a phantom model: comparison with conventional 64-detector row CT. *Int J Cardiovasc Imaging* 2012;28:337–42.
- [27] Jinzaki M, Yamada M, Tanami Y, et al. Evaluation of in-stent restenosis by high spatial resolution CT. *Curr Cardiovasc Imaging Rep* 2011;4: 431–6.
- [28] Prakash P, Kalra MK, Ackman JB, et al. Diffuse lung disease: CT of the chest with adaptive statistical iterative reconstruction technique. *Radiology* 2010;256:261–9.